AD-A142 460 THE CURVATURE PRIMAL SKETCH(U) MASSACHUSETTS INST OF TECH CAMBRIDGE ARTIFICIAL INTELLIGENCE LAB H ASADA ET AL. FEB 84 AI-M-758 N00014-75-C-0643 1/1

UNCLASSIFIED F/G 12/1 NL

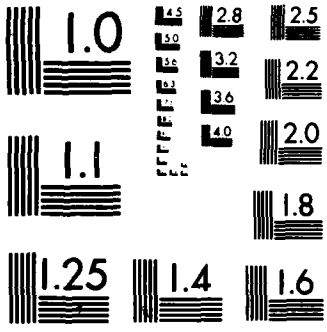

UNCLASSIFIED

SECURITY CLASSIFICATION OF THIS PAGE (When Data Entered)

REPORT DOCUMENTATION PAGE		READ INSTRUCTIONS BEFORE COMPLETING FORM
1. REPORT NUMBER AIM 758	2. GOVT ACCESSION NO.	3. RECIPIENT'S CATALOG NUMBER
4. TITLE (and Subtitle) The Curvature Primal Sketch		5. TYPE OF REPORT & PERIOD COVERED memorandum 6. PERFORMING ORG. REPORT NUMBER
7. AUTHOR(s) Haruo Asada and Michael Brady		8. CONTRACT OR GRANT NUMBER(s) N00014-75-C-0643 N00014-80-C-0505
9. PERFORMING ORGANIZATION NAME AND ADDRESS Artificial Intelligence Laboratory 545 Technology Square Cambridge, Massachusetts 02139		10. PROGRAM ELEMENT, PROJECT, TASK AREA & WORK UNIT NUMBERS
11. CONTROLLING OFFICE NAME AND ADDRESS Advanced Research Projects Agency 1400 Wilson Blvd Arlington, Virginia 22209		12. REPORT DATE February 1984 13. NUMBER OF PAGES 21
14. MONITORING AGENCY NAME & ADDRESS(if different from Controlling Office) Office of Naval Research Information Systems Arlington, Virginia 22217		15. SECURITY CLASS. (of this report) UNCLASSIFIED 15a. DECLASSIFICATION/DOWNGRADING SCHEDULE

16. DISTRIBUTION STATEMENT (of this Report)

Distribution of this document is unlimited.

17. DISTRIBUTION STATEMENT (of the abstract entered in Block 20, if different from Report)

18. SUPPLEMENTARY NOTES

None

19. KEY WORDS (Continue on reverse side if necessary and identify by block number)

Image understanding
vision
shape

20. ABSTRACT (Continue on reverse side if necessary and identify by block number)

In this paper we introduce a novel representation of the significant changes in curvature along the bounding contour of planar shape. We call the representation the curvature primal sketch. We describe an implemented algorithm that computes the curvature primal sketch and illustrate its performance on a set of tool shapes. The curvature primal sketch derives its name from the close analogy to the primal sketch representation advocated by Marr for describing significant intensity changes. We define a set of primitive para-

DD FORM 1 JAN 73 1473 EDITION OF 1 NOV 65 IS OBSOLETE

S/N 0102-014-6601

UNCLASSIFIED

SECURITY CLASSIFICATION OF THIS PAGE (When Data Entered)

Block 20 cont.

meterized curvature discontinuities, and derive expressions for their convolutions with the first and second derivatives of a Gaussian. The convolved primitives, sorted according to the scale at which they are detected, provide us with a multi-scaled interpre tation of the contour of a shape.

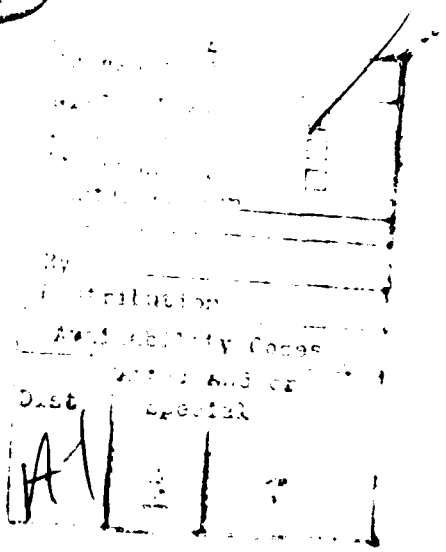

MASSACHUSETTS INSTITUTE OF TECHNOLOGY
ARTIFICIAL INTELLIGENCE LABORATORY

A. I. Memo 758 February, 1984

The Curvature Primal Sketch

Haruo Asada and Michael Brady

Abstract. In this paper we introduce a novel representation of the significant changes in curvature along the bounding contour of planar shape. We call the representation the *curvature primal sketch.* We describe an implemented algorithm that computes the curvature primal sketch and illustrate its performance on a set of tool shapes. The curvature primal sketch derives its name from the close analogy to the primal sketch representation advocated by Marr for describing significant intensity changes. We define a set of primitive parameterized curvature discontinuities, and derive expressions for their convolutions with the first and second derivatives of a Gaussian. The convolved primitives, sorted according to the scale at which they are detected, provide us with a multi-scaled interpretation of the contour of a shape.

Acknowledgements. This report describes research done at the Artificial Intelligence Laboratory of the Massachusetts Institute of Technology. Support for the laboratory's Artificial Intelligence research is provided in part by the Advanced Research Projects Agency of the Department of Defense under Office of Naval Research contract N00014-75-C-0643, the Office of Naval Research under contract number N0014-80-C-0505, and the System Development Foundation. This work was done while Haruo Asada was a visiting scientist at MIT on leave from Toshiba Corporation, Japan.

1. Introduction

Recently [Brady 1982a, 1982b, 1983, 1984a, Brady and Asada 1984], we have introduced a representation of two-dimensional shape called *smoothed local symmetries* (SLS). The (geometric aspects of the) representation are summarized in Figure 1. Figure 1a shows that both the bounding contour and the enclosed region of a shape are represented, for reasons discussed in [Brady and Asada 1984]. Figure 1b shows the hierarchical decomposition of a shape into subobjects. Smoothed local symmetries are being applied to recognition and inspection, and integrated with a system that can reason by analogy [Winston 1980, Winston, Binford, Katz, and Lowry 1984] to investigate the relationship between function and form [Brady 1984b].

The representation of the bounding contour of a shape, particularly of the significant changes of curvature, is called the *curvature primal sketch*, and it is the subject of this paper. There are three reasons for discovering and representing significant curvature changes. First, they amount to a rich, stable, description with local support that can enable the recognition of partially occluded objects. Second, they provide a set of knot points for constructing a perceptually close spline approximation to a contour. Finally, it is possible to describe a shape at multiple scales by interpreting the curvature events along the contour at various scales. The basic idea of the curvature primal sketch first appeared in [Brady and Asada 1984].

We call our representation the *curvature primal sketch*, because the representation of significant changes in curvature is analogous to the *primal sketch* representation of intensity changes in grey level images [Marr 1974, 1976]. For example, a discontinuity in the orientation of a tangent to the contour (C1 discontinuity) is perceived as a corner and is analogous to step changes in intensity. A discontinuity in curvature (C2 discontinuity) is a smooth junction of two pieces of contour and is analogous to a gradient edge.

Our approach follows that of Marr [1974]. We define a parameterized set of idealized curvature changes. The set includes composite structures such as end and crank (see Figures 8 and 9) which are analogous to thin bar and line ending respectively. We then derive expressions for the convolution of the primitives with the first and second derivatives of a Gaussian. The instances are described at a variety of scales in terms of the positions of the local maxima of the derivatives.

We use the idea of multiple scales in two ways. First, it is possible to find an instance of a curvature change primitive at one scale, even when it cannot be found at other scales. There are two main reasons for this. First, the filtered responses of two nearby curvature changes may be confounded at larger scales, and second, instances at smaller scales may be caused by noise. A pertinent observation, concerning intensity changes, but relevant because of the analogy between curvature and intensity changes, was made by Marr and Hildreth [1980] and Binford [1981], and discussed more explicitly by Canny [1983]. It is that there is an uncertainty principle between the detectability of an event and its accurate localization in the

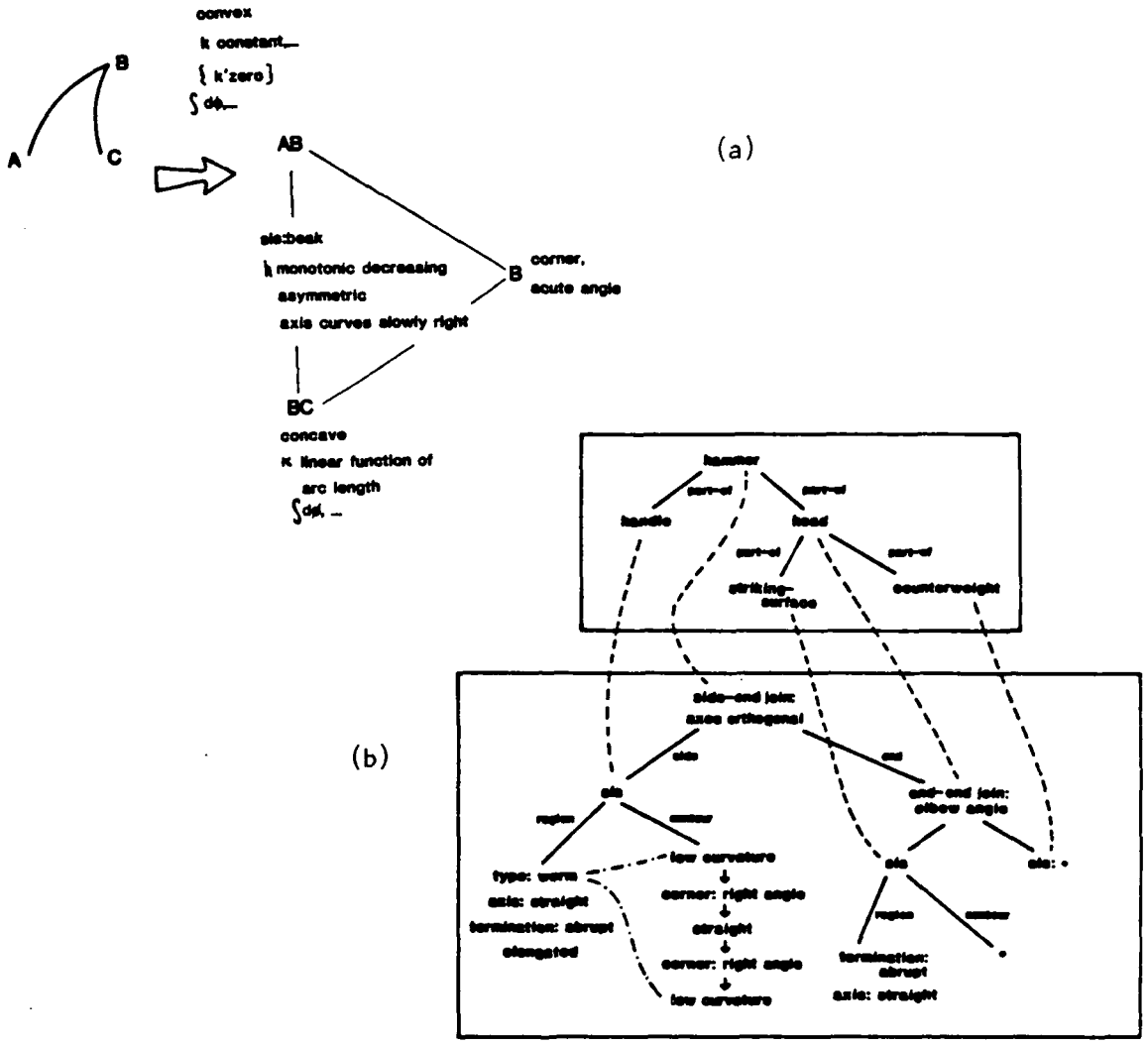

Figure 1. a. A portion of a shape and the corresponding smoothed local symmetry representation. The solid lines form the curvature primal sketch representation of the contour. The dotted lines form a representation of the region enclosed by the shape fragment. b. The representation of a hammer, showing the subparts. Other links form a ISA hierarchy, embody constraints, and detail the function of the shape. For details of smoothed local symmetries, see [Brady and Asada 1984].

presence of noise. That is, the coarser the edge finding operator, the more the signal to noise ratio (a measure of detectability of the event) is improved, while the smaller the operator, the more accurate the localization. By varying the width of an operator it is possible to vary the trade-off in signal to noise versus localization [Canny 1983]. Larger scales can be used for detecting the occurrence of events and smaller scales for localizing the events accurately.

We also use multiple scales in a second way, namely to build a multi-scaled description of a shape. The idea of convolving a signal with multiple operators

at different spatial scales has been explored for several years. Recently, however, Witkin [1983] has promoted the idea of *scale space*, a representation of a signal that consists of its convolution at multiple scales. An important part of Witkin's proposal is the automatic determination of the set of scales at which it is useful to describe a signal symbolically. Witkin's scale space representation is a ternary tree of zero crossings. He did not attempt to *interpret* the multiple descriptions in terms of primitive events as we have done.

Yuille and Poggio [1983a] have provided some theoretical underpinning for the scale space representation. They have shown that the contour of zero crossings of second derivatives ("fingerprint") may preserve enough information to reconstruct the original signal to within a constant scale factor. They also show [Yuille and Poggio 1983b] that a Gaussian filter is essentially unique in having the property that zero crossings are not introduced as one moves to coarser scales. However, as we discuss further below, this mathematical property cannot be relied on in an implementation of the interpretation process, since a discrete set of scales may make a match ambiguous when the responses of two nearby events are confounded. To our knowledge, the curvature primal sketch reported here is the first implementation of an interpretation process that generates multiple scale descriptions from multiple convolutions.

An instance of a curvature change primitive that is detectable at a large scale suggests that it is a dominant feature of the shape. One which is inhibited by a dominant event at a large scale and can be detected only at smaller scales indicates a feature that is geometrically less significant. However, geometrically less significant events are not necessarily less important for the successful execution of a vision task. A small dent in an object, for example, may be considered noise when the task is to identify the object, but it may be crucial when the task is to inspect for defects.

In section 2, we summarize the idea of the curvature primal sketch and define a set of primitives and their instances in scale space. Section 3 discusses the algorithm to build a multi-scale description. The results in the experiment on a set of tools are shown in Section 4.

2. Representing Significant Changes In Curvature

The contour of an object is represented by a spline whose knots are the significant changes in curvature. The smooth curves between the knots, what Perkins [1978] calls *concurves*, can be parameterized by approximating the portion of the contour linearly, with quadratics, cubics, Cornu spirals, or any other suitable function. Here we are more concerned with the problem of finding knots corresponding to curvature discontinuities than the parameterization of smooth portions of contour between knots. The detection and localization of discontinuities is more crucial because the good parameterization of a piece of contour depends on them (Figure 2).

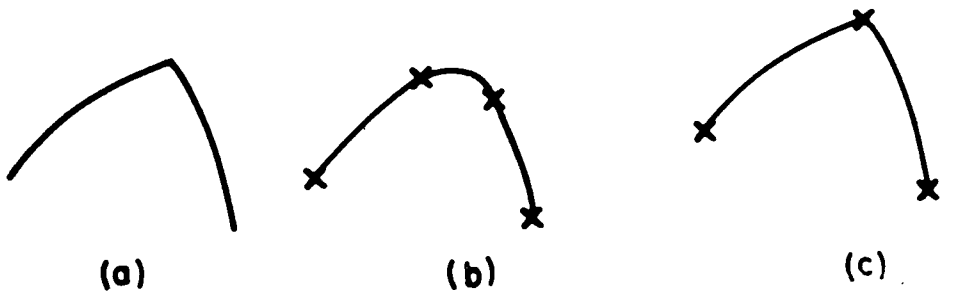

Figure 2. Knot points should mark significant changes of curvature along the contour. a. A corner fragment on a contour. b. Approximation when knot points (marked by crosses) are placed to either side of the perceived corner. c. Approximation when the corner is made explicit. (Reproduced from [Brady and Asada 1984, Figure 8])

In our experiments, piecewise circular approximation of the contour has proven to be good enough, provided we can first accurately locate all the semantically significant curvature changes as knots. In Figure 3a we show the contours of a number of tool shapes found by the Canny edge detector. Figure 3b shows the circular spline approximations to those contours once the curvature discontinuities have been located by the method described in this paper. Figure 3c shows the overlay of Figure 3b on Figure 3a.

We propose a particular set of primitive curvature changes. We analyze each primitive at several scales using an ideal parameterized version $f_i(s)$ of the primitive, where s denotes arc length along the contour. We then determine analytic forms for the convolutions of $f_i(s)$ with the first and second derivatives of Gaussian, namely $G'_\sigma * f_i$ and $G''_\sigma * f_i$, where G_σ denotes the Gaussian of standard deviation σ:

$$G_\sigma(t) = (1/\sqrt{2\pi}\sigma)\exp(-t^2/2\sigma^2).$$

Equivalently, by the derivative theorem of convolutions, we determine the analytic forms of $(G_\sigma * f_i(s))'$ and $(G_\sigma * f_i(s))''$. Then we construct a program to find instances of the curvature change models along actual contours.

2.1. Two Basic Discontinuities

We begin by deriving expressions for the convolutions of the two basic models, the corner and the smooth join, each of which have a single discontinuity. The convolutions of the compound models namely, crank, end, bump, and dent, are formed by appropriate superpositions of the filtered responses of these two models.

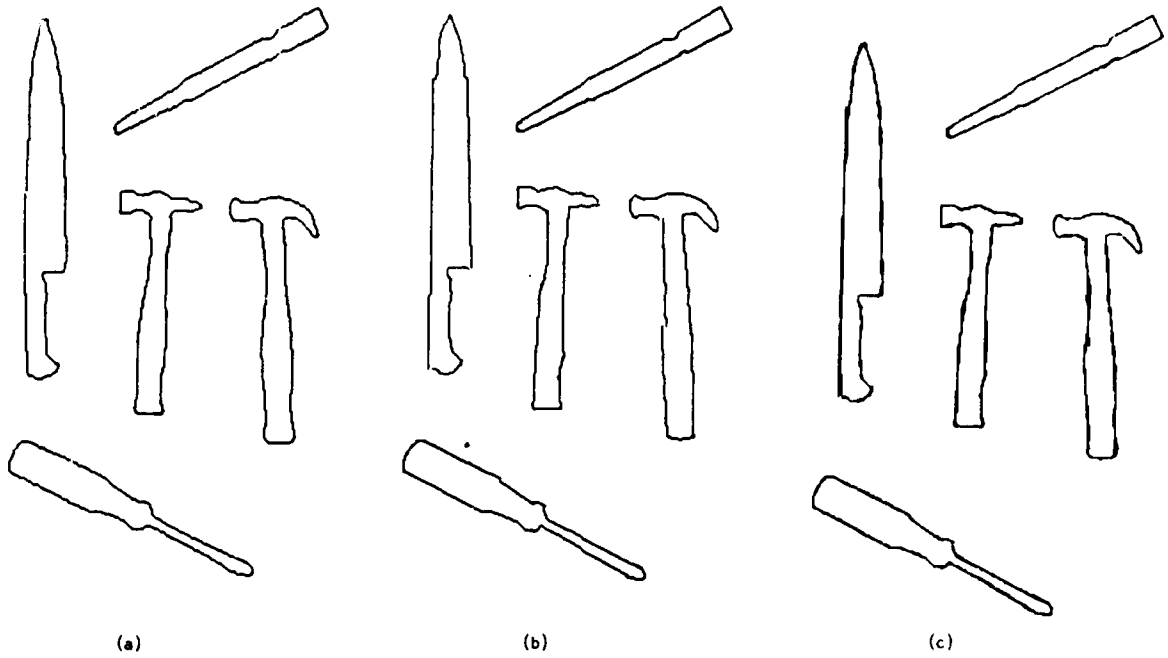

Figure 3. Illustrating the adequacy of circular splines for a set of tools. As discussed in Brady and Asada [1984], a circle may be replaced by a straight line depending on the condition number of the best fitting circle equations. a. The original contour. b. The circular spline approximation after finding the significant changes of curvature. c. Overlay of b on a.

1) Filtered response of a corner

Figure 4a shows a corner fragment consisting of two circular fragments of curvatures κ_1 and κ_2, enclosing an angular discontinuity of ϕ. Figure 4b shows the corner model in orientation space, relating the orientation of the tangent to the curve to arc length along the curve. The *corner* model is defined by:

$$f_{corner}(s) = \begin{cases} \kappa_1 s + c & \text{if } s < 0; \\ \kappa_2 s + c + \phi & \text{if } s > 0. \end{cases}$$

As we shall see, the convolutions of the model assume particularly simple forms when the curvatures of the circular arcs flanking the corner are the same, $\kappa_1 = \kappa_2 (= \kappa)$ say. We call that special case a *pure corner*. Its analytic form is:

$$f_{pc}(s) = \begin{cases} \kappa s + c & \text{if } s < 0; \\ \kappa s + c + \phi & \text{if } s > 0. \end{cases}$$

We now convolve f_{corner} with the Gaussian $G_\sigma(t)$, and find:

$$\sqrt{2\pi}\sigma(G_\sigma * f_{corner})(s) = \sqrt{2\pi}\sigma c + \phi\int_{-\infty}^{s} \exp(-\frac{t^2}{2\sigma^2})dt + \kappa_2 s\int_{-\infty}^{s} \exp(-\frac{t^2}{2\sigma^2})dt + \kappa_1 s\int_{s}^{\infty} \exp(-\frac{t^2}{2\sigma^2})dt + (\kappa_2 - \kappa_1)\sigma^2 \exp(-\frac{s^2}{2\sigma^2}).$$

It follows that

$$\sqrt{2\pi}\sigma(G_\sigma * f_{corner})'(s) = \phi\exp(-\frac{s^2}{2\sigma^2}) + \kappa_2\int_{-\infty}^{s} \exp(-\frac{t^2}{2\sigma^2})dt + \kappa_1\int_{s}^{\infty} \exp(-\frac{t^2}{\sigma^2})dt.$$

This has a particularly simple form for a pure corner namely:

$$\sqrt{2\pi}\sigma(G_\sigma * f_{pc})'(s) = \phi\exp(-\frac{s^2}{2\sigma^2}) + \sqrt{2\pi}\kappa\sigma.$$

The function $(G_\sigma * f_{pc})'(s)$ is shown in Figure 4c. It has the shape of a Gaussian that is offset from the line $\theta = 0$ by the scale and curvature dependent constant $\sqrt{2\pi}\kappa\sigma$ and is attenuated proportional to the angle ϕ.

Similarly, convolving with the second derivative of a Gaussian (approximately equal to a difference-of-Gaussians) yields:

$$\sqrt{2\pi}\sigma(G_\sigma * f_{corner})''(s) = \frac{-\phi}{\sigma^2} s\exp(-\frac{s^2}{2\sigma^2}) + (\kappa_2 - \kappa_1)\exp(-\frac{s^2}{2\sigma^2})$$

This function is shown in Figure 4d. It has a zero crossing near the corner separating two peaks of opposite sign. In the case of a pure corner, the expression assumes the following simple form:

$$\sqrt{2\pi}\sigma(G_\sigma * f_{pc})''(s) = \frac{-\phi}{\sigma^2} s\exp(-\frac{s^2}{2\sigma^2}).$$

The distance along the s-axis between the peaks is

$$d_{corner} = \frac{\sigma^2}{\phi}\sqrt{(\kappa_1 - \kappa_2)^2 + \frac{4\phi^2}{\sigma^2}}$$

In the case of a pure corner, this expression reduces to

$$d_{pc} = 2\sigma.$$

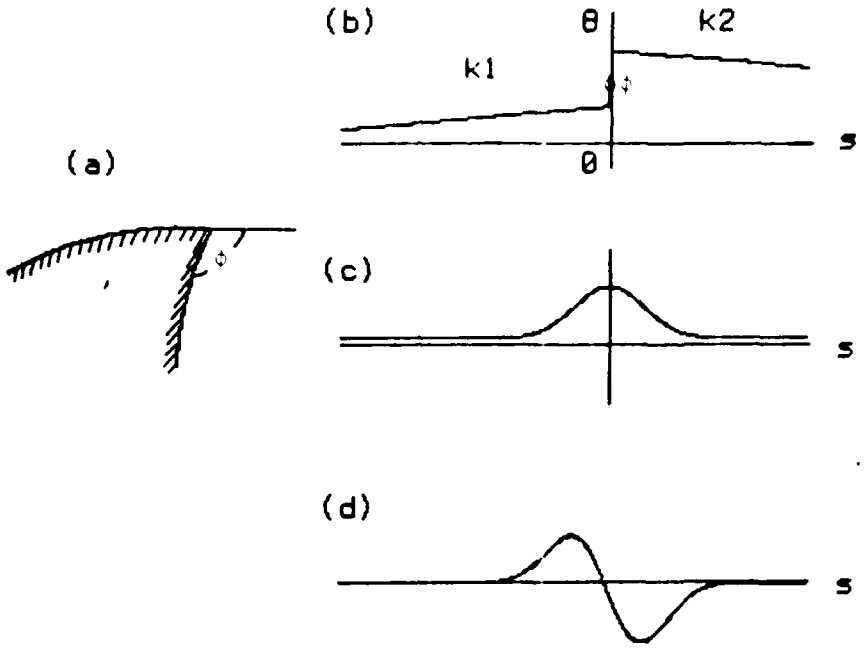

Figure 4. a. A corner fragment consisting of two circular fragments of curvatures κ_1 and κ_2, enclosing an angular discontinuity of ϕ. b. The corner model in orientation space, relating the orientation of the tangent to the curve to arc length along the curve. In the case of a pure corner, the slopes κ_1 and κ_2 are equal. c. The function $(G_\sigma * f_{pc})'(s)$. It has the shape of a Gaussian that is offset by the curvature κ and is attenuated proportional to the angle ϕ. d. The function $(G_\sigma * f_{corner})''(s)$, which corresponds to convolving the corner model with the second differential of a Gaussian. It has a zero crossing near the corner separating two peaks of opposite sign.

Note that d_{pc} is independent of ϕ and the pair of peaks merges when the scale gets smaller.

The formula for the heights of the side lobes is complex. In the special case $\kappa_1 = \kappa_2$, they are both equal to

$$h_{pc} = \frac{1}{\sqrt{2e\pi}} \frac{|\phi|}{\sigma^2}.$$

2) Filtered response of a smooth join

The corner model f_{corner} and its first derivative are discontinuous at the origin. If ϕ is set equal to zero, the orientation of the tangent is continuous, but the curvature is not. We call such a curvature change a *smooth join*. Figure 5a shows two instances of the model, whose defining equation is

$$f_{sj}(s) = \begin{cases} \kappa_1 s + c & \text{if } s < 0; \\ \kappa_2 s + c & \text{if } s > 0. \end{cases}$$

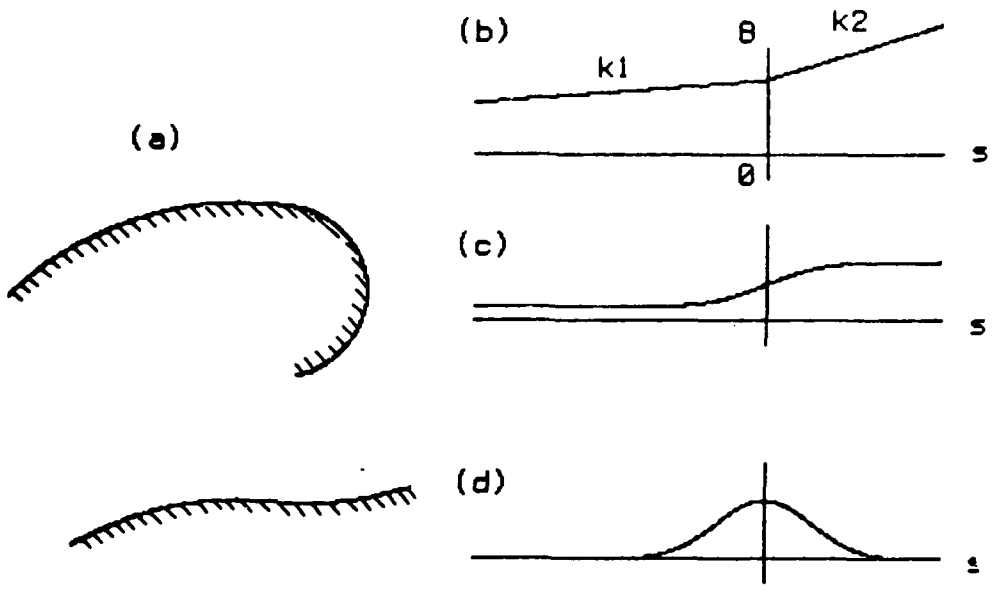

Figure 5. a. Two instances of a smooth join, in which the signs of the flanking curvatures are the same (top) and opposite (bottom). b. The smooth join in orientation space. c. The filtered response of a smooth join to the first derivative of a Gaussian. d. The filtered response of a smooth join to the first derivative of a Gaussian.

When the signs of the curvatures flanking the smooth join are opposite, the smooth join is called an *inflection*. Figure 5b shows the smooth join model in orientation space. It is well known that smooth joins are difficult to perceive unless there is a large difference $(\kappa_1 - \kappa_2)$ in the flanking curvatures. For example, Ullman [1976] and Brady, Grimson, and Langridge [1980] have investigated smooth curves that have a single C_2 discontinuity in curvature. Figure 6 shows a curve that is the smooth join of two circles. The curve and its tangent are continuous, but there is a step change in the curvature at a point along the curve. Evidently the curvature discontinuity is not perceived.

Inserting $\phi = 0$ into the equation for the response of a corner to the first derivative of a Gaussian, we find

$$\sqrt{2\pi}\sigma(G_\sigma * f_{sj})'(s) = \kappa_2 \int_{-\infty}^{s} \exp(-\frac{-t^2}{2\sigma^2})dt + \kappa_1 \int_{s}^{\infty} \exp(-\frac{-t^2}{\sigma^2})dt.$$

Suppose, without loss of generality, that $\kappa_1 < \kappa_2$. Then

$$\sqrt{2\pi}\sigma(G_\sigma * f_{sj})'(s) = \kappa_1\sigma\sqrt{2\pi} + (\kappa_2 - \kappa_1)\int_{-\infty}^{s} \exp(-\frac{-t^2}{2\sigma^2})dt$$

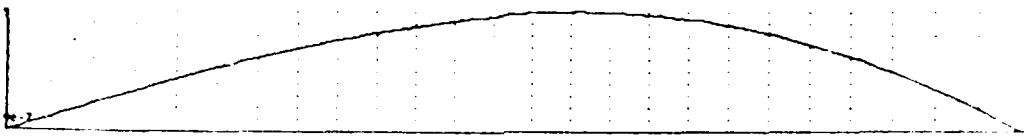

Figure 6. Two circular arcs smoothly joined. Reproduced from Brady, Grimson, and Lancaster 1980, Figure 2.

This function is shown in Figure 5c. It has the form of a smooth step whose height is proportional to $(\kappa_1 - \kappa_2)$, the difference in curvatures flanking the join. If the difference in flanking curvatures is small the step may not be perceived.

Differentiating again, we find the filtered response of the smooth join to a second differential of a Gaussian.

$$\sqrt{2\pi}\sigma(G_\sigma * f_{sj})''(s) = (\kappa_2 - \kappa_1)\exp(-\frac{s^2}{2\sigma^2}).$$

This response is shown in Figure 5d. It has a single peak whose height is proportional to $(\kappa_2 - \kappa_1)/\sigma$. Introducing the quantity $\phi_{sj} = (\kappa_2 - \kappa_1)\sigma\sqrt{e}$, we can write an expression for the height of the response peak that is similar to the expression for the height of the peaks in the corner response, namely

$$h_{sj} = |\phi_{sj}|/\sigma^2\sqrt{2\pi e}.$$

The detectability of a smooth join is essentially determined by the peak height h_{sj}, that is by the value of ϕ_{sj}. In particular, a smooth join is hard to detect unless the product of σ and $(\kappa_2 - \kappa_1)$ is sufficiently large. This is consistent with human perception of changes such as those indicated in Figure 6. It is not known how the threshold on ϕ_{sj} required to perceive a smooth join is related to that on ϕ required to perceive a corner.

2.2. Primitive curvature changes and their detection

In this section, we introduce the five primitive curvature changes that we use in the curvature primal sketch. We call them corners, smooth joins, cranks, ends, and bumps or dents. We define each primitive and show it in orientation space. We show example responses at different scales when the primitive is filtered with the second derivative of a Gaussian. Corners and smooth joins were analysed in the previous section; in this section we show different scale responses and give detection criteria.

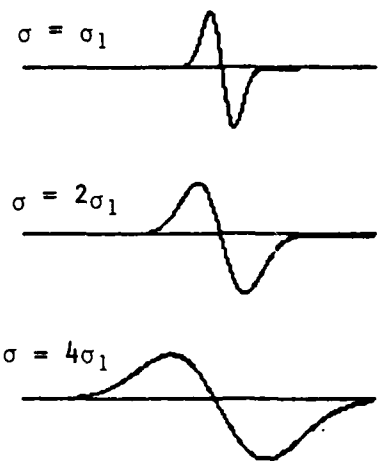

Figure 7. The responses to the corner shown in Figure 4 to $(G''_\sigma$ at several spatial scales σ.

The corner primitive

As shown in Figure 4d, a corner gives rise to a pair of peaks whose separation is d_{corner}. An expression h_{pc} for the heights of the peaks was given for the case of a pure corner. If the flanking curvatures κ_1 and κ_2 are not equal, so that there are simultaneous C_1 and C_2 discontinuities, the zero crossing in $(G''_\sigma * f_{corner})(s)$ is not exactly at the origin. In practice, the difference $\kappa_1 - \kappa_2$ is small, so that $d_{corner} \approx d_{pc}$. Note that d_{corner} is linearly dependent on the scale constant σ, and hence it monotonically decreases with σ. This provides a strong clue for recognition of corners and enables spatially close events to be decomposed in order to distinguish a pair of smooth joins from a corner. Figure 7 shows the second derivative filtered responses to a corner at several scales.

The smooth join primitive

In the previous section, we showed that the response of a smooth join to the first derivative of a Gaussian is a smooth step, and that to the second derivative it is a peak. The peak height is $(\kappa_2 - \kappa_1)/(\sigma\sqrt{2\pi})$. Recall that only when the curvatures flanking the smooth junction are very different can this be reliably found. Inflections produce a zero crossing in the first derivative response.

The end primitive

An end consists of two corners with angle changes of the same sign (Figures 8a and 8b). It is not necessary that the contour fragments comprising the end are straight or parallel, nor are the corners required to be right angles. An end is analogous to the primal sketch intensity change called a "line ending" [Marr 1976]. Let a be the distance along the contour between the corners forming the end. At large (dimensionless) scales, when the ratio σ/a is greater than one, the filtered responses of the contributing corners are confounded, and the end is perceived as a corner. At smaller scales, when the ratio σ/a is less than a half, the individual

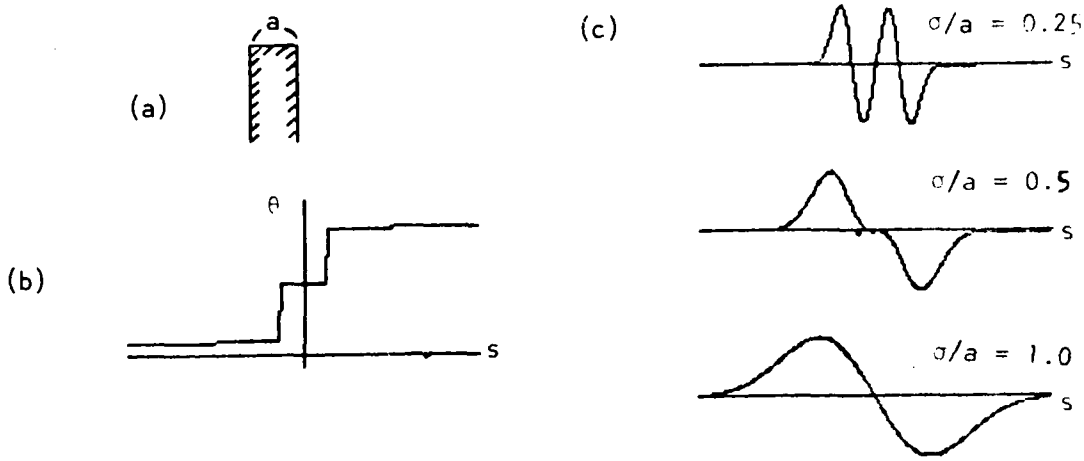

Figure 8. a. A typical end as it appears on a contour. b. The end in orientation space. c. the second derivative filtered responses to an end at several (dimensionless) scales.

corner responses are separated, enabling the detection of the corner pair. This occurs, for example, in the interpretation of end_1 for the punch shape shown in Figure 11. Figure 8c shows the second derivative filtered responses to an end at several (dimensionless) scales.

The crank primitive

A crank is like an end, except that the changes in angle are of opposite sign (Figures 9a and 9b). It is analogous to the primal sketch intensity change called a "thin bar" [Marr 1976]. Again let a be the arc length between the corners forming the crank. When the ratio σ/a is less than one half, the crank is essentially signalled by two independent corner responses. When σ/a is greater than one, a crank produces a strong central peak with two side peaks of opposite sign that are at most half the height of the central peak if curvature differences are negligible. Figure 9c shows second derivative filtered responses to a crank at several (dimensionless) scales.

The bump and dent primitives

Instances of a bump and dent are shown in Figure 10a and Figure 10b. They are typically spatially localized and correspond to two nearby cranks of opposite sign. Figure 10c shows filtered responses at several scales. They are reliably detected by finding the sequence of four peaks at a suitably small scale.

Different instances of the primitives at suitably coarse scales can be ambiguous. Figure 11 shows several ambiguous contour fragments. An example of the ambiguity

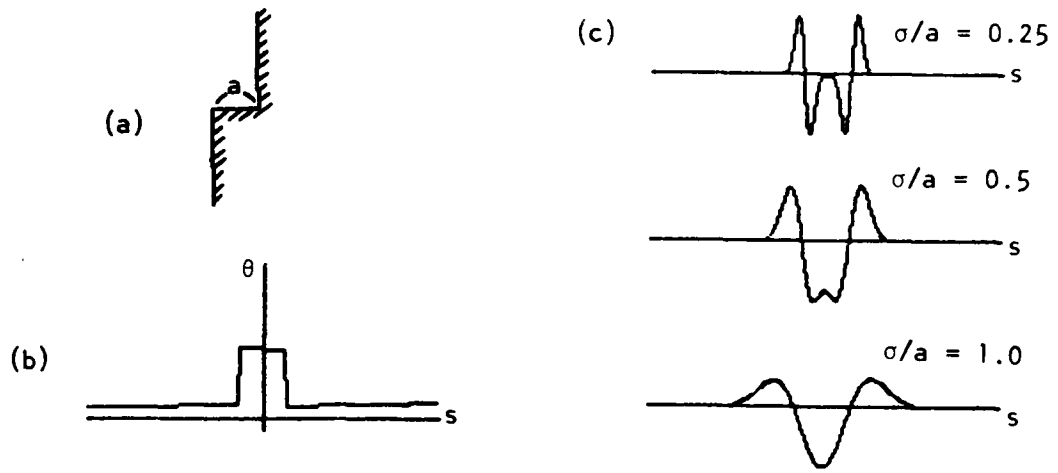

Figure 9. a. A typical crank as it appears on a contour. b. The crank in orientation space. c. the second derivative filtered responses to an crank at several (dimensionless) scales.

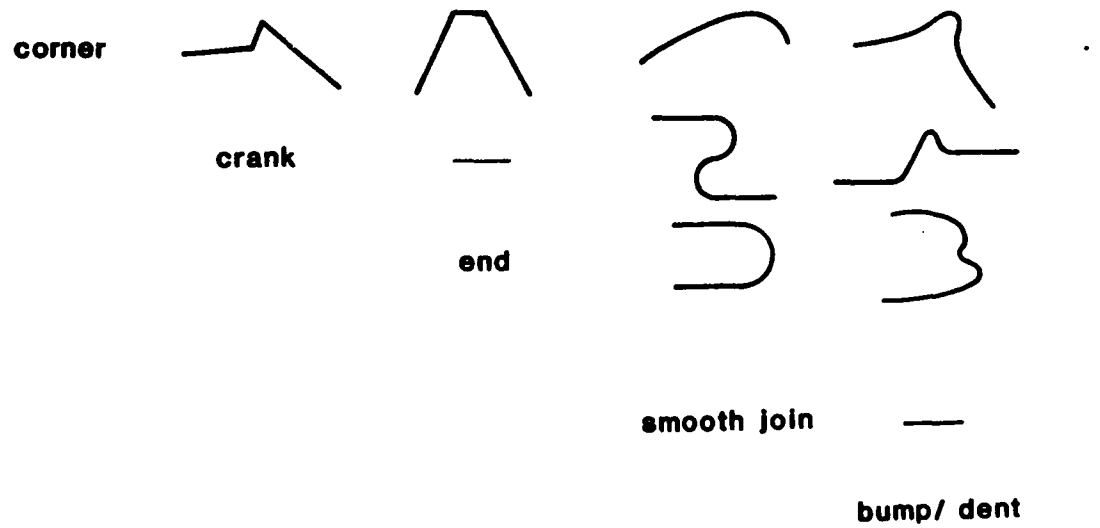

Figure 11. A matrix of contour fragments that appear ambiguous at suitable scales.

between a crank and a smooth join will be found in the curvature primal sketch of a screwdriver in Figure 19.

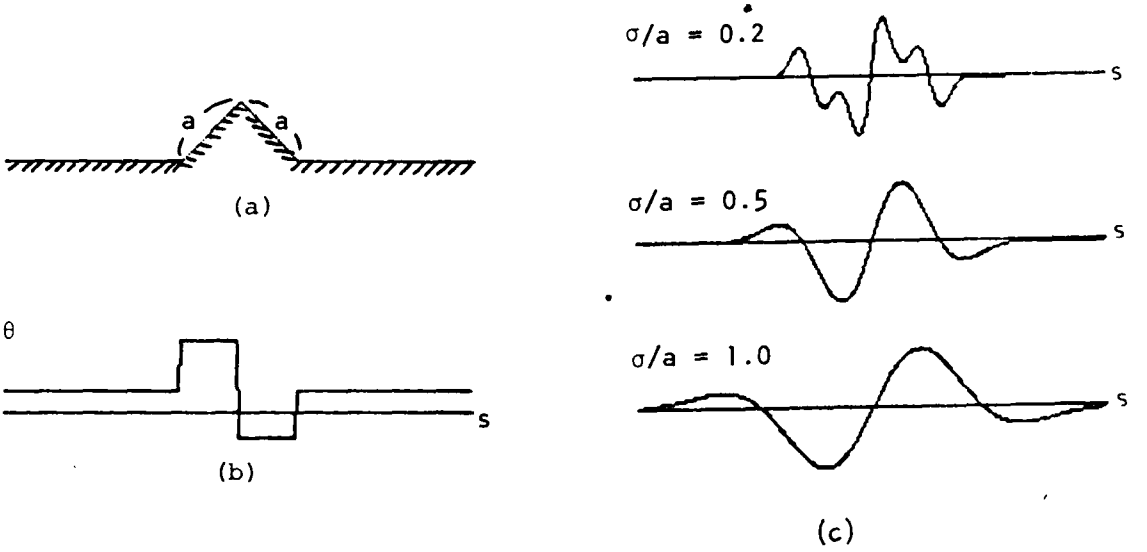

Figure 10. a. A typical bump as it appears on a contour. b. The bump in orientation space. c. the second derivative filtered responses to a bump at several (dimensionless) scales.

3. MultiscaleInterpretation

In this section we describe an implemented algorithm that produces a multi-scale curvature primal sketch representation of a contour.

Step 1: Convolving orientation with derivatives of Gaussians

The bounding contour of a shape is found using the edge finder developed by Canny [1983]. The filtered responses $G'_\sigma * c(s)$ and $G''_\sigma * c(s)$ are computed for the contour $c(s)$ at a variety of scales σ. The result is a set of one dimensional arrays for both G'_σ and G''_σ. Figures 12 through 15 show examples for four tool shapes.

Step 2: Matching the Locations of Peaks among Scales

The locations of local positive maxima and local negative minima in the filter responses computed in step 1 are extracted and matched among the scales, producing a tree. Ideally, the tree is equivalent to a "fingerprint" [Yuille and Poggio 1983]. However, we cannot trust the tree entirely because the match can be ambiguous for two nearby events. For example, each of the two peaks that signal an end splits into a pair of peaks when the ratio σ/a is one. However, due to the discretization of the scale factor and the effect of the curvature difference between two fragments of the contour, it is possible that only one of the peaks splits into two at a particular scale. In such cases, the match between the new peak and the old ones is ambiguous. We need knowledge of the primitive type in order to build

a complete tree, but such knowledge is not available until the tree is interpreted. Consequently, it is necessary to leave the tree incomplete and take it into account at the interpretation stage.

Step 3: Parsing the tree

The parsing method we use is simple. In the early stages of this research, we considered using heuristic methods, such as relaxation and dynamic programming, in order to cope with the ambiguity that occurs at the interpretation of the responses of two closely located events. However, it has turned out that in the vast majority of cases these responses can be decomposed easily by looking at the movement of the peaks over several scales and taking account of the convergence property of a corner response. This experience supports idea of scale space as a representation technique.

Instances of the composite structures, namely ends, bumps and cranks are searched for first. The movement of the peaks at lower scales and the heights of the peaks are the only clues for the detection. Once an instance is detected, the tree is refined. The search proceeds to lower scales until the scales are exhausted. Next, corners are searched for in the same manner and finally inflections and smooth junctions.

Step 4: Computing Knot Points

Instances of curvature primitives detected by the parsing process are represented by a part of the tree starting with a peak at the scale at which the instance was first detected. The exact position of each primitive, which gives rise to knot points on the contour, is computed from the tree. For corner primitives, the zero crossing between peaks at the smallest scale gives good localization. For smooth joins, on the other hand, good localization is accomplished at the largest scale. The primitives, sorted according to the scale, provide us with a multi-scale interpretation of the contour.

4. Examples

In this section we show some examples of the multi-scaled interpretation of a contour. The results are for the set of tools shown in Figures 12 through 15.

Figure 16 shows how the curvature primal sketch procedure works on the shape of the punch shown in Figure 12. Figure 16a shows the positions of the local positive maxima (+) and negative minima (-) in the first derivatives (top) and second derivatives (bottom). Connecting lines are the part of the tree which was generated when an instance was found. At the largest scale, $\sigma = 22$, two ends are found. Then a dent at the scale of 11, two cranks at $\sigma = 8$, and another dent at $\sigma = 5$ are detected. Figure 16b illustrates the multiple scale interpretation of the shape. It starts out as a trapezium and its fine structure becomes clear as scale gets smaller.

Similarly, Figure 17 shows the curvature primal sketch representation of the carving knife shown in Figure 13. Figure 17a is similar to Figure 16a. At the largest

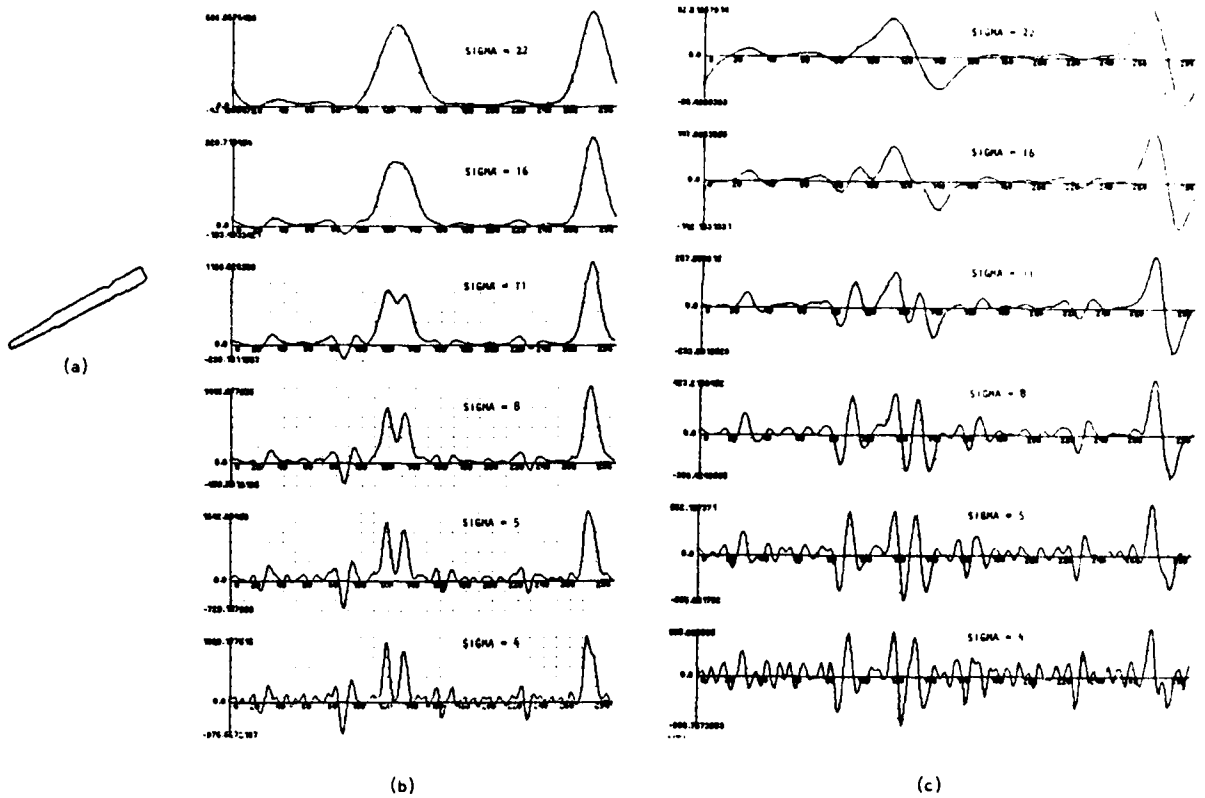

Figure 12. a. The contour of a punch or nail set. b. The filtered responses with G'_σ. c. The filtered responses with G''_σ.

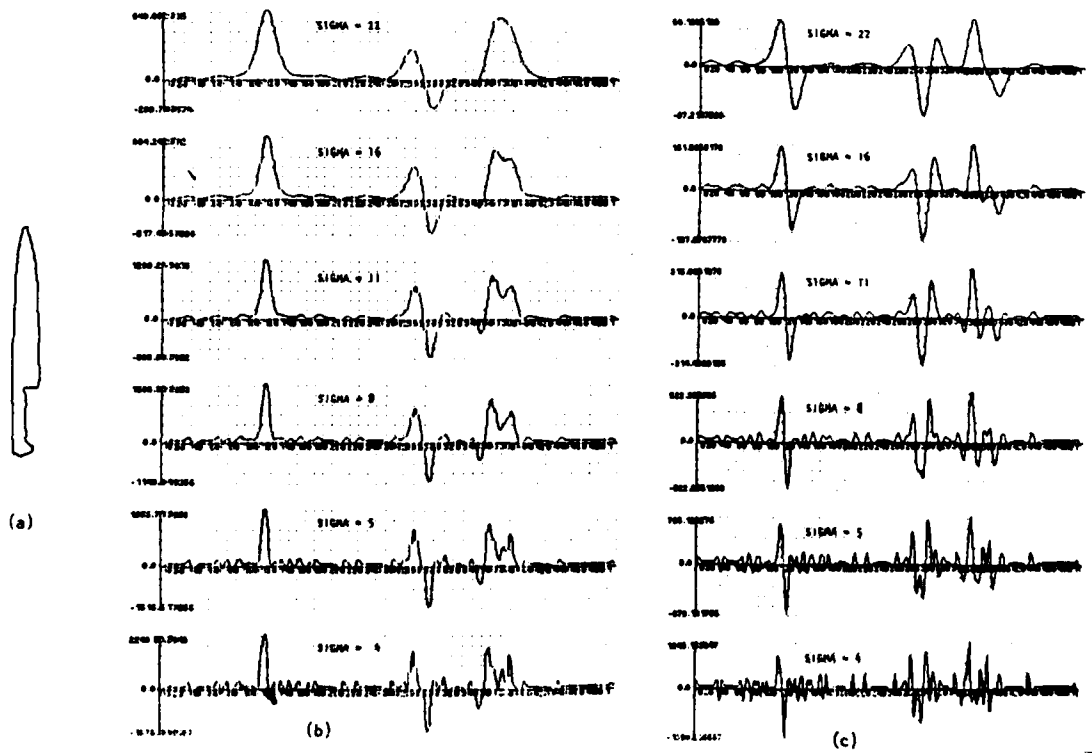

Figure 13. a. The contour of a carving knife. b. The filtered responses with G'_σ. c. The filtered responses with G''_σ.

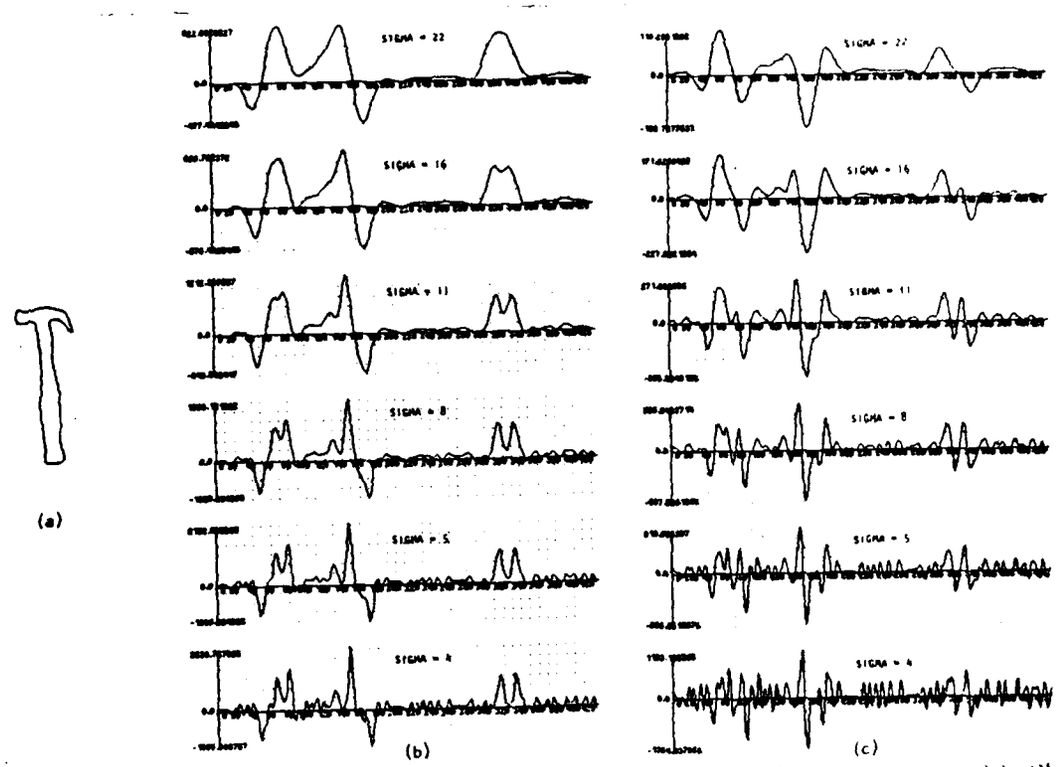

Figure 14. a. The contour of a Warrington hammer. b. The filtered responses with G'_σ. c. The filtered responses with G''_σ.

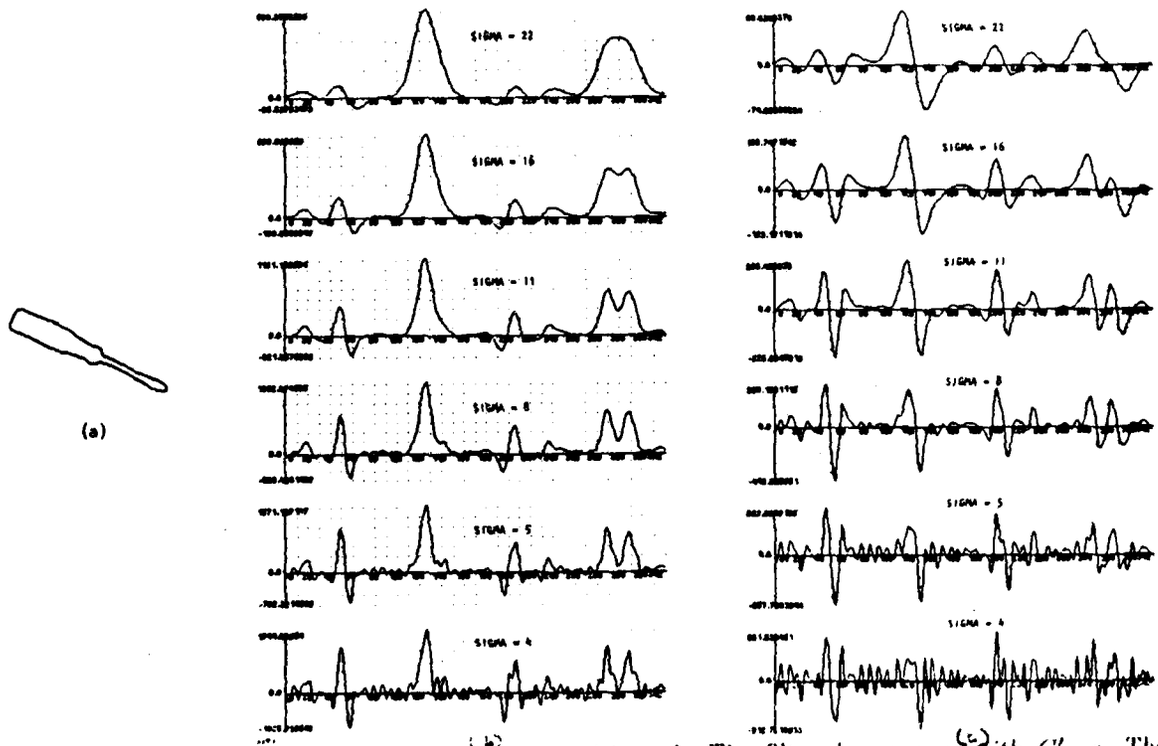

Figure 15. a. The contour of a screwdriver. b. The filtered responses with G'_σ. c. The filtered responses with G''_σ.

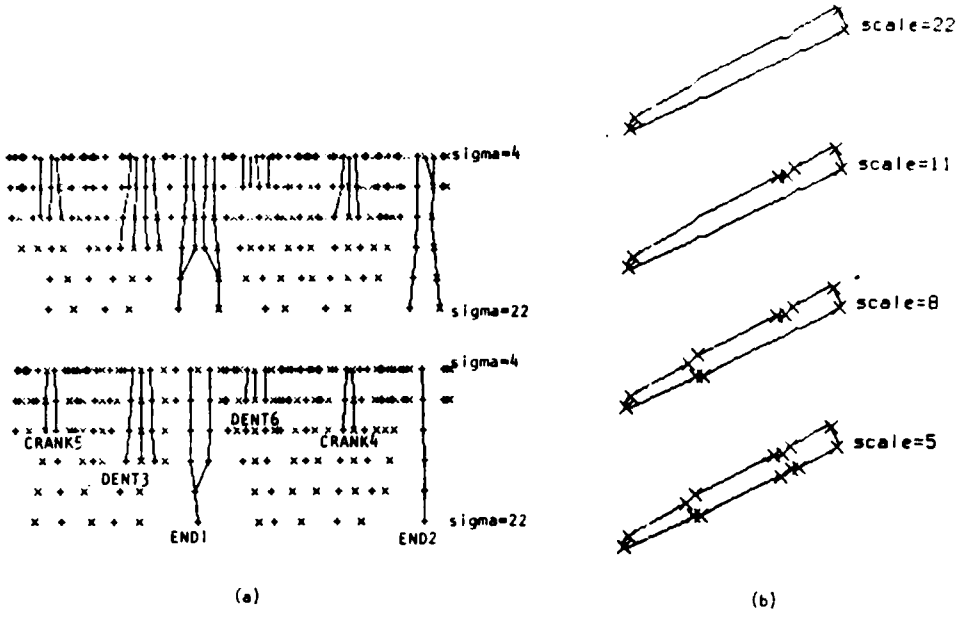

Figure 16. a. The positions of the local positive maxima (+) and negative minima (-) in the first derivatives (top) and second derivatives (bottom) for the filtered responses of the punch (Figure 12). Connecting lines are the part of the tree which was generated when an instance was found. b. The multiple scale interpretation of the shape.

scale, again $\sigma = 22$, all the major curvature discontinuities are found. These are the tip of the blade, the crank signalling the join of the blade and handle, and the hand grip at the end of the handle. At finer scales, smooth joins are found on the blade and the handle. These would occur in different positions in different views of the knife (see below).

Figure 18a shows the local extrema of the filtered responses for the Warrington hammer shown in Figure 14. At the largest scale, the following discontinuities are discovered: the end of the handle, the corners defining the side-end join of the handle and head of the hammer, the end signalling the striking surface on the head, the tip of the nail puller, and a smooth join on the nail puller. At smaller scales additional smooth joins are found, first on the head and then on the handle. At the largest scale, the description of the handle is that it is a cylinder (a "worm" in the terminology of Blum and Nagel [1976]). At a smaller scale, a pair of inflections, symmetric about the axis of the handle, is found. The corresponding description of the handle is that it has a thick body and a thinner neck. Heide [1984, forthcoming] shows how to generate symbolic descriptions of this sort from smoothed local symmetries (Hollerbach [1975] has shown how rich symbolic descriptions can be generated from an appropriate geometric analysis of a shape).

Figure 19a shows the filtered responses of the screwdriver shown in Figure 15. At the coarsest scale, the end of the blade, the corners defining the end of the handle, and the pair of cranks signalling the join of the handle and the blade are all discovered. At scale $\sigma = 11$, an inflection is found on the handle. The symmetrically placed discontinuity, a crank, is not found until the scale is 8. Note

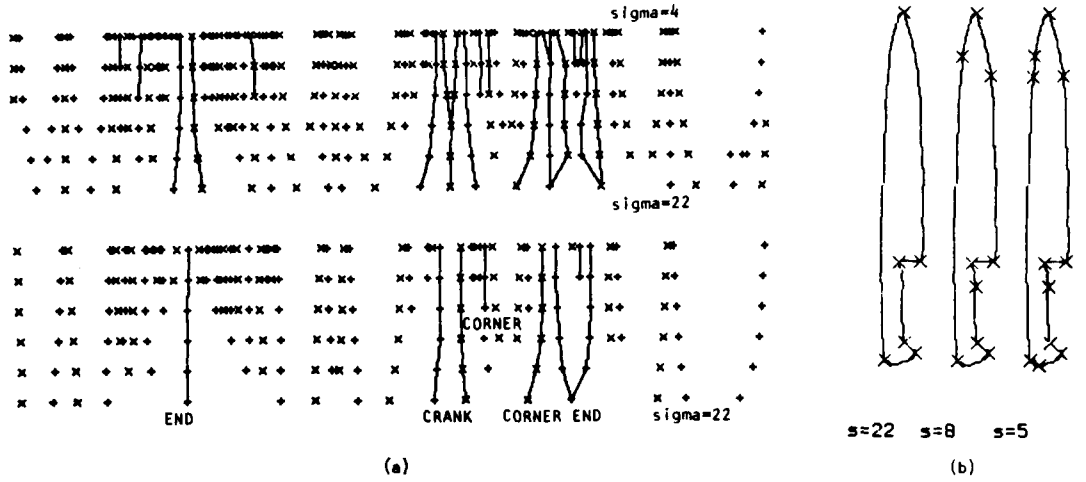

Figure 17. a. The positions of the local positive maxima (+) and negative minima (-) in the first derivatives (top) and second derivatives (bottom) for the filtered responses of the carving knife (Figure 13). Connecting lines are the part of the tree which was generated when an instance was found. b. The multiple scale interpretation of the shape.

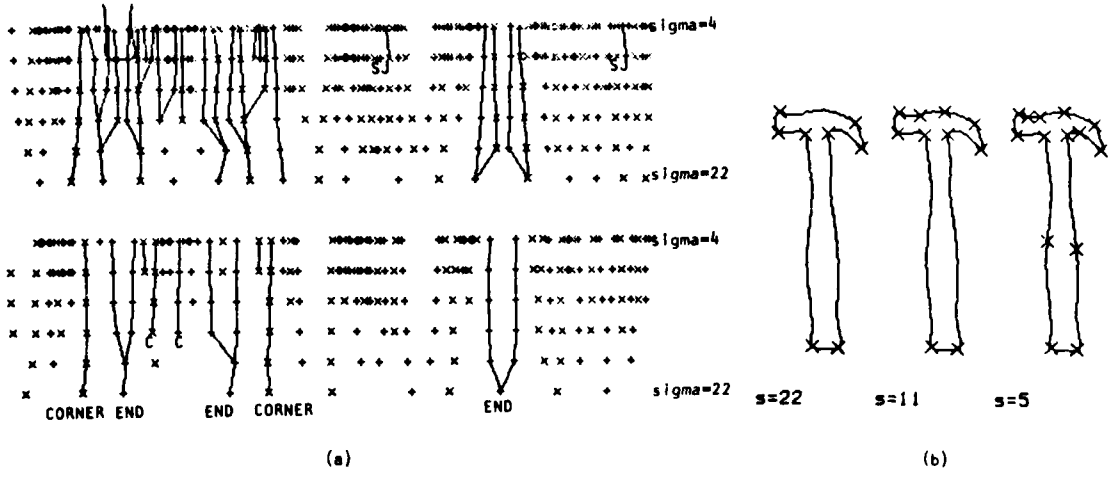

Figure 18. a. The positions of the local positive maxima (+) and negative minima (-) in the first derivatives (top) and second derivatives (bottom) for the filtered responses of the Warrington hammer (Figure 14). Connecting lines are the part of the tree which was generated when an instance was found. b. The multiple scale interpretation of the shape.

that an inflection and a crank are ambiguous at certain scales, as noted earlier.

We finally illustrate the robustness of our algorithm. In Figure 20 each shape is the bounding contour of the same object as the screwdriver shown in Figure 19

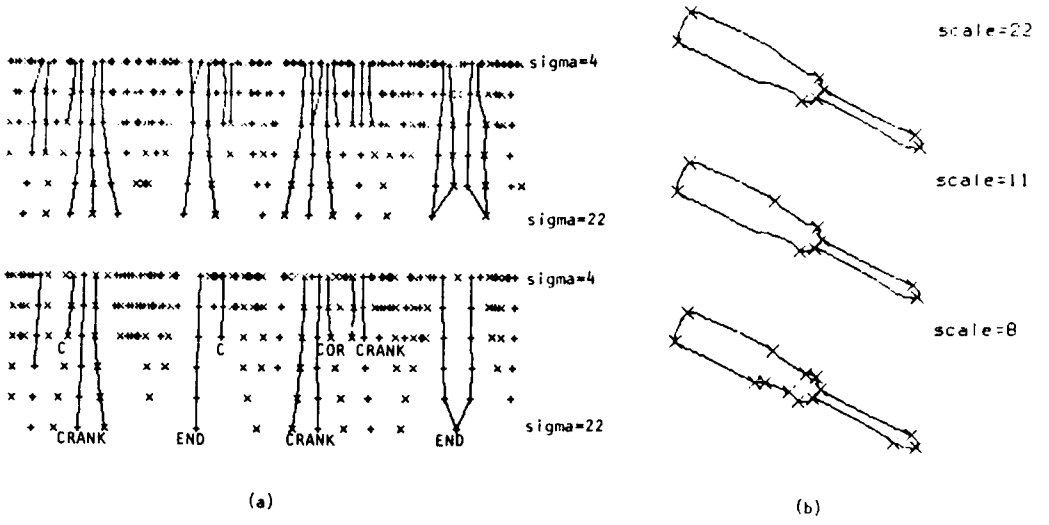

Figure 19. a. The positions of the local positive maxima (+) and negative minima (-) in the first derivatives (top) and second derivatives (bottom) for the filtered responses of the screwdriver (Figure 15). Connecting lines are the part of the tree which was generated when an instance was found. b. The multiple scale interpretation of the shape.

but the orientation is different. Due to noise in the imaging process and directional tesselation, each is slightly different. However, the interpretation is still reasonable. In each case, the two ends are stably detected. Also, the two cranks that signal the join of the handle and shaft are found at the same scale. Other cranks at the grip are also found in all cases though at different scales.

5. Conclusion

In this paper we have discussed the problem of computing a representation of the significant changes in curvature, and shown that it is possible to produce multi-scale representation of a contour by interpreting the significant changes in curvature at various scales. Our method applies more generally to any one-dimensional signals when an appropriate set of primitives is chosen, because the problem of representing a 1-D waveform can be reduced to two subgoals; segmenting the whole signal into homogenous (in some sense) portions and parameterizing them. This is exactly the same as our problem.

The result shown in this paper can be used for developing the region- and contour-based representation of 2-D shape [Brady 1984a]. We can also use the symbolic interpretation as clues for finding subpart joins without the knowledge of the object's identity.

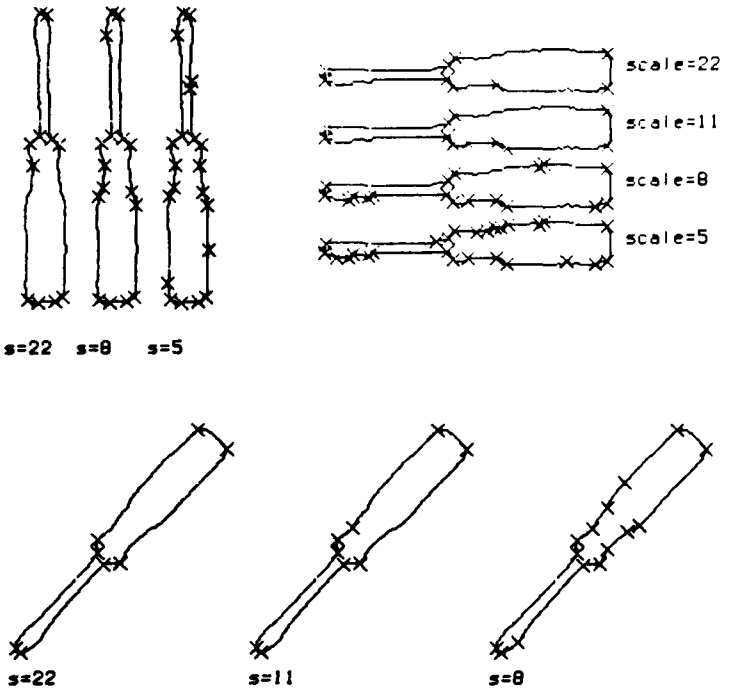

Figure 20. Knot points for the screwdriver(Fig.5c) with different orientation.

6. Acknowledgements

Many colleagues commented on earlier drafts or presentations of the material in this paper. We thank especially Steve Bagley, Bob Bolles, John Canny, Marik Ghallab, Georges Giralt, Laurent Gouzenes, Scott Heide, Tommy Poggio, Patrick Winston, and Alan Yuille.

7. References

Binford, Thomas O., [1981], "Inferring Surfaces from Images," *Artificial Intelligence*, **17**, 205 - 244.

Brady, J. Michael, [1982a], "Parts Description and Acquisition Using Vision," *Robot Vision, Rosenfeld A. (ed.) SPIE*, 20 - 28.

Brady, J. Michael, [1982b], "Smoothed Local Symmetries and Local Frame Propagation," *Proc. Patt. Rec. and Im. Proc., Las Vegas, June*, , 629 - 633.

Brady, Michael, [1983], "Criteria for representations of shape," *Human and Machine Vision, Beck J., Hope, B., and Rosenfeld A. (eds.), Academic Press.*

Brady, Michael, [1984a], "Representing Shape," *Proc. of IEEE Int. Conf. on Robotics, Atlanta*, .

Brady, Michael, [1984b], "Artificial Intelligence and Robotics," *To appear.*

Brady, Michael, Grimson, W. E. L., and Langridge D. J, [1980], "Shape encoding and subjective contours," *Proc. First AAAI Conf., Stanford, August*, 15–17.

Brady, Michael, and Haruo Asada, [1984], "Smoothed Local Symmetries and Their Implementation," *The First International Symposium on Robotics Research, eds. Brady, Michael, and Paul. R. P., MIT Press, Cambridge, Mass.*

Canny, John Francis, [1983], "Finding Edges and Lines in Images," *MIT Artificial Intelligence Lab. TR-720.*

Marr, David, [1974], "The Low-Level Symbolic Representation of Intensity Changes in an Image," *MIT Artificial Intelligence Laboratory AIM-325.*

Marr, David, [1976], "Early Processing of Visual Information," *Phil. Trans. Royal Society of London* **B, 275**, 483 - 524.

Marr, D. and Hildreth, E.C, [1980], "Theory of Edge Detection," *Proc. R Soc. Lond. B,* **270**, 187-217.

Perkins, W. A., [1978], "A Model-Based Vision System for Industrial Parts," *IEEE Trans. Computer,* **C-27, (2)**, 126 - 143.

Ullman, S, [1976], "Filling in the gaps: the shape of subjective contours and a model for their generation," *Biol. Cyb.*, **25**, 1 – 6.

Winston, Patrick H, [1980], "Learning and reasoning by analogy," *Comm. ACM,* **23**.

Winston, Patrick H., Binford, Thomas O., Katz, Boris, and Lowry, Michael, [1984], Learning physical descriptions from functional descriptions, examples, and precedents.

Witkin, A., [1983], "Scale-Space Filtering," *Proc. 7th Int. Jt. Conf. Artif. Intell., Karlsrühe,* 1019 - 1021.

Yuille, A.L. and Poggio, T, [1983a], "Fingerprints Theorems for Zero-Crossings," *MIT Artificial Intelligence Laboratory AIM-730.*

Yuille, A.L. and Poggio, T, [1983b], "Scaling theorems for zero crossings," *MIT Artificial Intelligence Laboratory AIM-722.*